Mimicry of the proton wire mechanism of enzymes inside a supramolecular capsule enables β-selective O-glycosylations

Authors: Tian-Ren Li,[1,2] Fabian Huck,[1,2] GiovanniMaria Piccini,[3] and Konrad Tiefenbacher[1,2,4]*.

[1]Department of Chemistry, University of Basel, Mattenstrasse 24a, 4058 Basel, Switzerland

[2]NCCR Molecular Systems Engineering, BPR 1095, Mattenstrasse 24a, CH-4058 Basel, Switzerland

[3]Facoltà di Informatica, Istituto Eulero, Università della Svizzera Italiana (USI), Lugano, Switzerland

[4]Department of Biosystems Science and Engineering, ETH Zurich, Mattenstrasse 26, 4058 Basel, Switzerland

*email: konrad.tiefenbacher@unibas.ch / tkonrad@ethz.ch.

Abstract: Enzymes achieve high substrate and product selectivities by orientating and activating the substrate(s) appropriately inside a confined and finely optimized binding pocket. Enzyme catalysis is generally regarded as the ultimate role model for chemical catalysis, and some basic aspects of enzymes have already been mimicked successfully with man-made catalysts. One fascinating facet of substrate activation inside enzyme pockets, which has not been mimicked with man-made catalysts so far, involves proton wires. A proton wire facilitates the dual activation of a nucleophile and an electrophile via a reciprocal proton transfer, enabling highly stereoselective reactions under mild conditions. Here we present evidence for such an activation mode inside the supramolecular resorcin[4]arene capsule and demonstrate that it enables catalytic and highly β-selective glycosylation reactions. Extensive control experiments provide very strong evidence that the reactions take place inside the molecular container. The communicating dual activation mode enabled by the proton wire is, to our knowledge, unknown in supramolecular and molecular catalysis so far.

Enzymes have functioned as role models for chemists working in the broad field of catalysis. They enable conversions in an aqueous environment by binding the substrate(s) inside a hydrophobic binding pocket. The finely optimized environment of such binding pockets facilitates the highly selective conversion by orientating and activating the substrate(s) appropriately. Some aspects of enzymes, for instance, the binding pocket, have already been mimicked successfully with

supramolecular catalysts. Early work by Breslow, Sanders, Cram, Diederich, and others focused mainly on covalently modified cyclodextrins, cyclic porphyrin oligomers, spherands, and cyclophanes.[1-3] An alternative approach that requires less synthetic work utilizes the self-assembly of smaller building blocks to form discrete molecular cages and capsules.[4-8] Molecular capsules, first reported by Rebek in the early 1990s,[9] are self-assembled, closed host structures that allow the reversible binding of guest molecules. Molecular cages are structurally related but feature openings large enough for solvent and, usually, also guest exchange. It has been demonstrated that the entrapment inside capsules and cages can lead to different reactivities and selectivities compared to regular solution chemistry.[5,7,10-23] One fascinating facet of substrate activation inside enzyme pockets, which has not been mimicked with man-made catalysts so far, involves proton wires. Proton wires enable the facile transfer of protons over long distances via hydrogen bonds. For instance, the two active sites of the enzyme complex pyruvate dehydrogenase communicate with each other via the transfer of a proton over a wire of approx. 20 Å in length.[24] The proton wire consists of acidic amino acid side chains and water molecules which are linked via hydrogen bonds. This sophisticated non-covalent connection enables efficient proton transfer via a process that is often referred to as the "Grotthuss mechanism".[25] Recently, in 2015, an inverting cellulase enzyme was studied in detail using neutron diffraction and high-resolution x-ray diffraction analysis, which enabled the visualization of the detailed hydrogen bond network.[26] It was found that a proton wire connects the nucleophile (water, red arrow in Fig. 1A) with the general acid (Asp^{114}, green arrow) that activates the electrophile (glycosidic oxygen). The electrophile requires a general acid, while the nucleophile depends on a general base for deprotonation. A reciprocal proton transfer over a multitude of bonds, enabled via the proton wire, satisfies the requirements of both reaction partners for activation (light blue bold circular arrow in Fig. 1A), enabling the stereoselective reaction under mild conditions without the need for a strongly acidic activation agent. Such a communicating dual activation mode is, to our knowledge, unknown in supramolecular and molecular catalysis so far. Here we present evidence for such an activation mode inside the supramolecular resorcin[4]arene capsule **I** (Fig. 1B) and demonstrate that it enables highly β-selective glycosylation reactions.

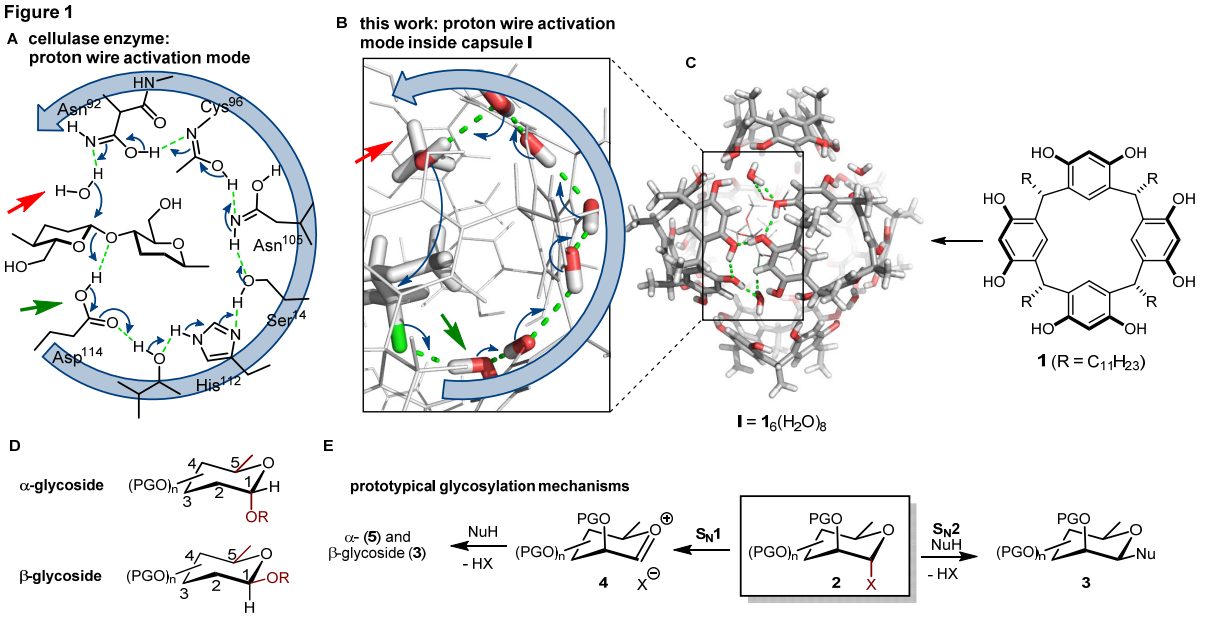

Figure 1. (A) Active site of an inverting cellulase enzyme.[26] A proton wire connects the nucleophile (water, red arrow in Fig. 1A) with the general acid (Asp^{114}, green arrow) that activates the electrophile (glycosidic oxygen). (B) We report that the supramolecular capsule **I** enables a similar activation mode inside its binding pocket. The catalyst activates the nucleophile (red arrow) and electrophile (green arrow), and synchronizes both reaction partners via seven hydrogen bonds. These seven hydrogen bonds are depicted as green dotted lines. (C) Catalyst **I** self-assembles from six resorcin[4]arene units **1** and eight water molecules. (D) Glycosides exist in the α- and the thermodynamically less stable β-form. (E) Prototypical S_N1 or S_N2 mechanisms for the glycosylation reactions.

The hexameric capsule **I**, originally reported by the Atwood group,[27] self-assembles via hydrogen bonds from six resorcin[4]arene units **1** and eight water molecules in apolar solvents (Fig. 1C).[28-30] The first two examples for catalysis inside **I** were reported by the groups of Reek and Scarso.[31,32] Subsequently, our group,[11] and others[12] utilized the capsule for the catalysis of a variety of reactions. Although **I** itself exhibits decent Bronsted acidity (pKa approx. 5.5),[33] a strong Bronsted acid co-catalyst (HCl) is required for several reactions.[34] However, even in these cases, the reactions take place inside the cavity, presumably via a proton shuttle mechanism.[35] Inspired by a report from Aoyama[36] in 1990 on the formation of methyl β-ribofuranoside from ribose using superstoichiometric amounts of resorcin[4]arene **1**, we investigated the possibility of performing glycosylation reactions inside capsule **I**. One main challenge in glycosylation chemistry remains

the stereoselective formation of the glycosidic linkage that can yield two isomers; the α-isomer featuring the glycosidic bond *anti* to the substituent at C5 (Fig. 1D), and the thermodynamically less stable β-isomer with its *syn* relationship. Although tremendous progress has been achieved,[37-46] the stereoselective chemical synthesis of carbohydrates remains challenging.[47] While the glycoside donor (electrophile) with the leaving group in α-configuration is readily available stereoselectively due to its thermodynamic stability, its stereoselective conversion is challenging. Conceptually, two different reaction pathways are possible (Fig. 1E): A clean S_N2 pathway would deliver β-product **3** selectively. In contrast, the S_N1 pathway with its cationic intermediate **4** would usually lead to α/β mixtures. In practice, however, the stereoselective substitution at the anomeric carbon is much more complex since a wide continuum of mechanisms between these two prototypical cases has been observed.[48] The exact pathway is influenced by all reaction parameters involved; not only the solvent, concentration, temperature, catalyst/activating agent, and the nucleophile, but also all aspects of the substrate itself: its substitution and the configuration of the substituents, its conformation that is strongly influenced by the protecting groups utilized, and also the leaving group. Although numerous methods have been developed, usually many different parameters have to be optimized to achieve excellent selectivity. A general approach to β-glycosides exists for glycoside donors (electrophiles) featuring an equatorially configured ester group at C2. Due to neighbouring group participitation, high β-selectivity for the glycosylation can be obtained, delivering *trans*-1,2-β-products. However, *cis*-1,2-, and 2-deoxy-β-products are not accessible via such a neighboring group effect. In 2017, the Jacobsen group reported an approach that allows the catalytic β-selective construction of a wide range of glycosidic linkages, including the challenging *cis*-1,2-, and 2-deoxy-products, utilizing a macrocyclic bis-thiourea catalyst.[49,50] We here report, that the communicating dual activation mode discovered in capsule **I**, enables a rather general β-selective glycosylation, that is only limited by the cavity size.

Results and discussion

An initial screening revealed that the chloride leaving group displayed promising reactivity in combination with capsule **I**. Exposing tetra-O-methyl-α-D-glucosyl chloride **6** (Fig. 2A; 0.10 M in chloroform, with neutral aluminum oxide (alox) as HCl scavenger) to 5 eq. methanol for 8 h in the presence of 10 mol% capsule, delivered the methyl glycoside **7** in 79% isolated yield and excellent β-selectivity (α:β $< 5:95$). The high β-selectivity was surprising. To further optimize the

reaction conditions, the challenging permethylated α-D-mannosyl chloride **8** (Fig. 2B) was utilized as the glycoside donor (see SI chapter 4 for details). Due to its C2-substituent being in an axial orientation, β-selective glycosylation is not only electronically but also sterically disfavored.[38] Interestingly, the same reaction conditions were successful; only the temperature was reduced from 30 °C to 20 °C as it slightly increased the *dr*. Under these conditions, the product formed in 11:89 α:β-selectivity and was isolated in good yield (75%). Even higher selectivities were obtained with the permethylated α-mannosyl *fluoride* **10** as the donor (Fig. 2C). Although glycosyl fluorides are very stable donors,[51] an excellent 7:93 α:β-selectivity and a good yield (74%) were obtained at only slightly elevated temperature (50 °C), but otherwise identical reaction conditions.

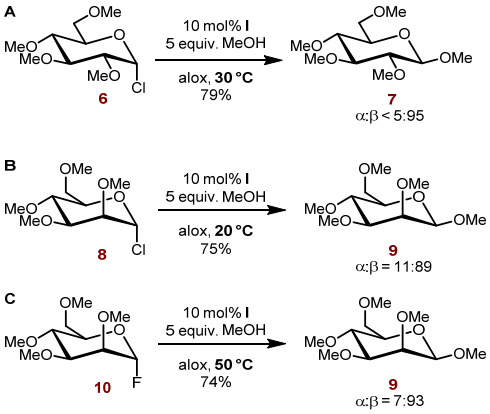

Figure 2. Summary of the screening results. (A) Initial results with glycosyl chloride **6**. (B) The same conditions (at a reduced temperature, 20 °C) were also applicable to the challenging mannosyl chloride **8** with its C2-substituent in the axial position. (C) An even higher selectivity was observed for the mannosyl fluoride **10** (7:93); for details see SI chapter 4.

Control experiments

The unusually high β-selectivity obtained for the glycosylation of the three substrates (**6**, **8**, and **10**, Fig. 2) indicates that the glycosylation takes place inside the cavity of **I**. In solution, such a selectivity would not be expected as extensive research has demonstrated.[37-45] Indeed, without the capsule catalyst, under otherwise identical conditions, only a 7% yield of a diastereomeric product mixture (α/β = 43:57) and some hydrolysis product was observed (Fig. 3A, entry 2). Nevertheless, a series of further control experiments were performed to learn more about the role of the capsule catalyst. Blocking the cavity of **I** with an excess of a high-affinity guest (Et_4NBF_4),[32] should

efficiently prevent the glycosylation reaction from taking place inside the capsule (Fig. 3A, entry 3). Only small amounts of a diastereomeric product mixture (α/β = 44:56) were formed, presumably mainly outside of **I**. Disassembling the catalyst, either via the addition of DMSO (entry 4) or by the use of acetone as a polar solvent (entry 5), prevented product formation in good selectivity, or even completely. The same was true when capsule **I** was replaced by the closely related hexameric pyrogallolarene (**PG**) capsule **II** (entry 6; see Fig. 3B for structure of **PG** and the corresponding capsule **II**).[52,53] Although the substrates were encapsulated inside **II** (see SI, page S11), no formation of the glycoside product was observed. This control experiment will be discussed in the context of the reaction mechanism (next chapter) in more detail. Also attempts of replacing **I** with a structural subunit, 4-hexylbenzene-1,3-diol, unable to assemble to a capsule, failed to reproduce the high yields and selectivities (entry 7). The same was true when replacing the mildly acidic capsule catalyst **I** with Bronsted or Lewis acids under otherwise identical reaction conditions. Even in a larger excess (200 mol%), only a trace of conversion was observed with acetic acid (entry 8) or trifluoroacetic acid (entry 9). The use of superstoichiometric amounts of boron trifluoride led to an acceptable conversion (51% yield, entry 10), however, like the other acids employed, failed to induce diastereoselectivity.

All results obtained are consistent with the β-selective glycosylation taking place inside the cavity of catalyst **I**. If the reaction takes place inside the closed cavity, a substrate size selectivity should be obtainable. Therefore, size competition experiments were performed. In the first set of experiments, the α-configured glucosyl chloride **6** was reacted with a 1:1-mixture of differently sized nucleophiles (methanol and 1-docosanol, Fig. 3C). Under capsule catalysis, only the methyl glycoside **7** was detectable by ^{1}H-NMR, and as expected was obtained in excellent β-selectivity. Under regular solution conditions (200 mol% $BF_3.Et_2O$, $CDCl_3$, 50 °C) both nucleophiles reacted, to deliver a product mixture in a ratio of approx. 60:40 (**7**/**11**). Both of these products were formed as α/β-mixtures in ratios of 58:42 and 45:55, respectively. In the second set of experiments, a mixture of differently sized glycosyl donors (**6** and **12**) was utilized (Fig. 3D). While capsule catalysis delivered the smaller product **13** exclusively, and in excellent β-selectivity, the solution experiment again delivered mixtures. These experiments provide very strong additional evidence that the high β-selectivity stems from a reaction inside the capsule and not on the outer surface, or in solution. To the best of our knowledge, there is no alternative man-made catalyst available that selectively glycosylates mixtures of donors or acceptors of similar reactivity that only differ in

size. Furthermore, the reaction does not suffer from significant product inhibition as demonstrated for glucosyl chloride **6** and methanol (see SI chapter 7).

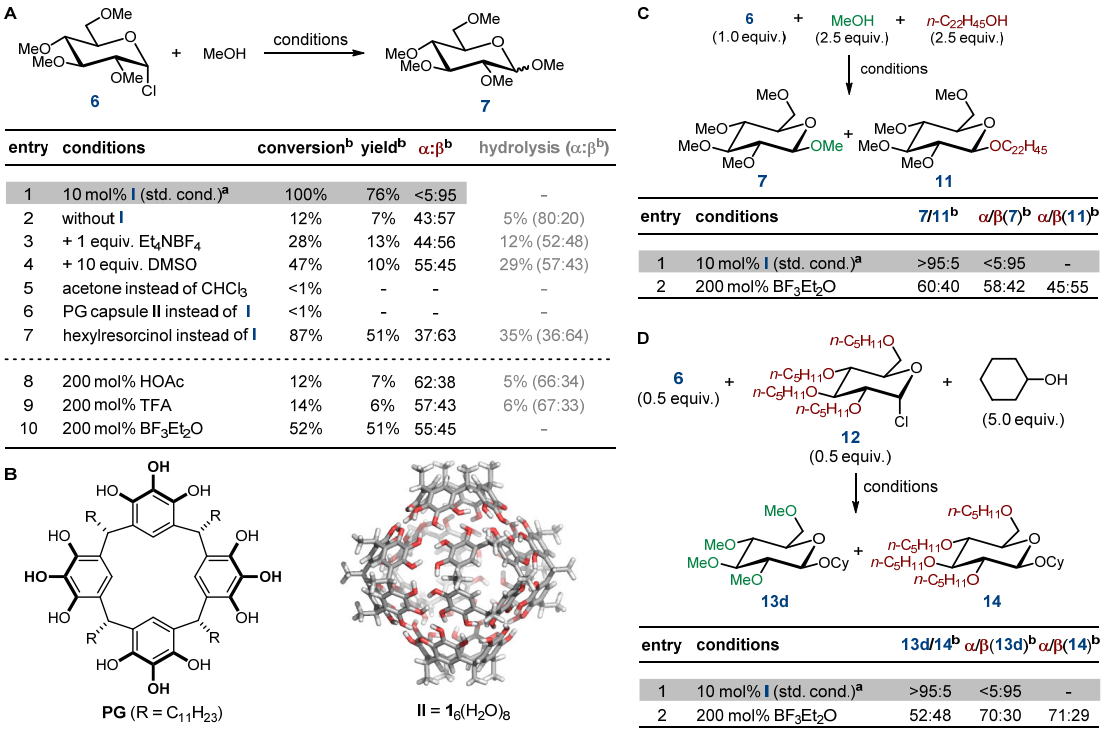

entry	conditions	conversion[b]	yield[b]	α:β[b]	hydrolysis (α:β[b])
1	10 mol% **I** (std. cond.)[a]	100%	76%	<5:95	-
2	without **I**	12%	7%	43:57	5% (80:20)
3	+ 1 equiv. Et_4NBF_4	28%	13%	44:56	12% (52:48)
4	+ 10 equiv. DMSO	47%	10%	55:45	29% (57:43)
5	acetone instead of $CHCl_3$	<1%	-	-	-
6	PG capsule **II** instead of **I**	<1%	-	-	-
7	hexylresorcinol instead of **I**	87%	51%	37:63	35% (36:64)
8	200 mol% HOAc	12%	7%	62:38	5% (66:34)
9	200 mol% TFA	14%	6%	57:43	6% (67:33)
10	200 mol% BF_3Et_2O	52%	51%	55:45	-

entry	conditions	7/11[b]	α/β(7)[b]	α/β(11)[b]
1	10 mol% **I** (std. cond.)[a]	>95:5	<5:95	-
2	200 mol% BF_3Et_2O	60:40	58:42	45:55

entry	conditions	13d/14[b]	α/β(13d)[b]	α/β(14)[b]
1	10 mol% **I** (std. cond.)[a]	>95:5	<5:95	-
2	200 mol% BF_3Et_2O	52:48	70:30	71:29

Figure 3. Control experiments concerning the role of the capsule catalyst. (A) Different reaction conditions that prevent reactions inside the capsule (entries 2-7), and regular solution reactions (entries 8-10) failed to induce high β-selectivities. (B) Structures of pyrogallolarene (**PG**) and the corresponding capsule **II** utilized in A, entry 6. (C) A size competition experiment with two different nucleophiles was performed and indicated that a high β-selectivity can be obtained only inside the capsule catalyst. (D) A size competition experiment with two different donors was performed, indicating that a high β-selectivity can be obtained only inside the capsule catalyst. [a]standard reaction conditions for glycosyl chloride [10 mol% capsule, $CDCl_3$, 30 °C, alox as additive]; [b]determined by ^1H NMR analysis of the reaction mixture.

Mechanistic investigations

To learn more about the glycosylation mechanism inside capsule **I**, several experiments were performed. First, the dependence of the stereochemical outcome on the electrophile configuration was explored. Due to their superior stability, the α- and β-*fluorinated* glucosyl donors were

prepared in pure anomeric form. While invertive substitution was observed with the α-configured glucosyl fluoride α-**15** (72% yield, α:β = 6:94, Fig. 4A), the β-configured donor β-**15** delivered an anomeric mixture of the product with a small preference for the α-isomer (54% yield, α:β = 64:36, Fig. 4B). Furthermore, kinetic investigations were performed. For the determination of the secondary kinetic isotope effect (SKIE), the deuterated substrate D-α-**15** (Fig. 4C) was prepared (see SI, page S6). An SKIE value of 1.19 ± 0.021 (50 °C), corresponding[54] to a value of 1.21 (25°C), was determined from the H/D ratios in the isolated product and starting material (see SI, page S85). However, the interpretation of the value is not straightforward when comparing with other literature values. Values of 1.16-1.20 (23 °C) were interpreted as consistent an intermediate with "significant oxo-carbonium ion character"[55] or a "loose S_N2 transition state".[56] Therefore, we decided to investigate the reaction order of the nucleophile methanol (Fig. 4D). Interestingly, close to the standard reaction concentration of methanol (0.50 M), approx. zero-order in methanol was observed. The slightly negative trend likely stems from the destabilization of the capsule via the polar additive methanol. However, at lower methanol concentrations (0.025 – 0.100 M), a first order in methanol was observed. First order was also observed for the glycosyl fluoride substrate α-**15** over the whole concentration range investigated (see SI page S67). The first order in methanol observed excludes a potential S_N1 mechanism, while the approx. zero-order at higher methanol concentrations indicates saturation of the capsule with methanol, likely via incorporation into the hydrogen bond network.[57] Based on the SKIE and the zero reaction order of methanol observed, the very high β-selectivity most likely stems from a loose S_N2-mechanism. For the α-configured substrate (Fig. 4A), the S_N2 inversion takes place efficiently providing very high to quantitative inversion. However, for the β-configured substrate β-**15** (Fig. 4B), the S_N2 mechanism is stereoelectronically disfavored, providing only reduced invertive α-selectivity.

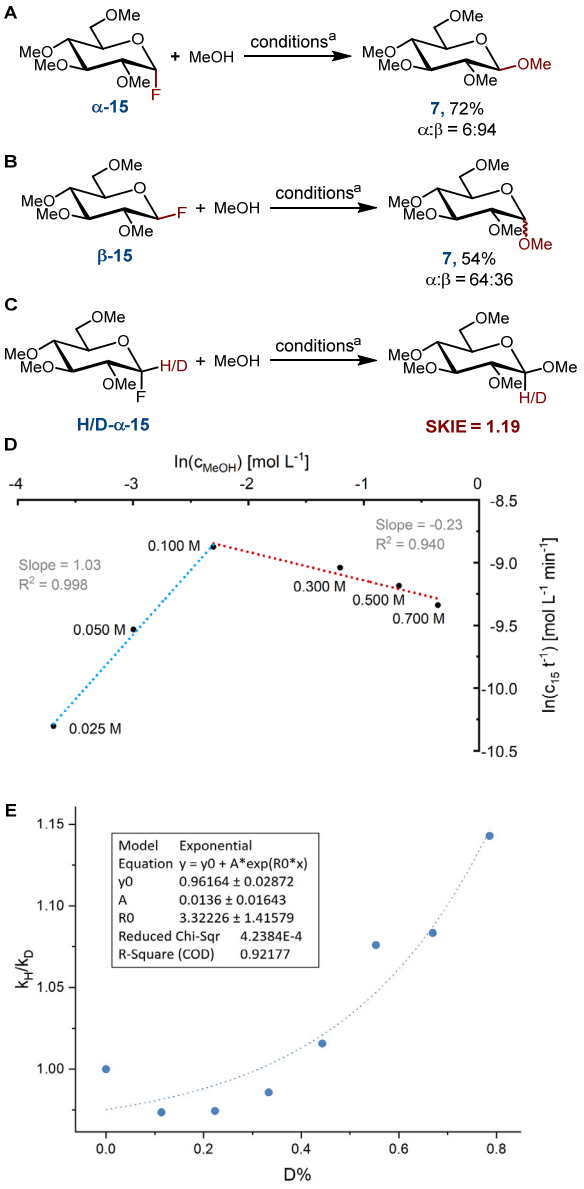

Figure 4. Mechanistic Investigations. (A) An invertive substitution was observed for the α-configured glucosyl fluoride α-**15**. (B) A substantially reduced invertive selectivity was observed for the β-configured glucosyl fluoride β-**15**. (C) The SKIE was determined from a competition experiment of a mixture of regular α-**15** and its deuterated analog at low conversion (23%). (D) Logarithmic plot of the initial rate of product formation versus methanol concentration. The slope of the trend line represents the order of the reaction. For methanol concentrations < 0.100 M the reactions show first-order behavior. Concentrations > 0.100 M lead to a saturation-like behavior, the negative slope likely stems from a partial disassembly of the capsule at higher methanol

concentrations. (E) Proton inventory study for the conversion of **α-15**. [a]standard reaction conditions for glycosyl fluoride [10 mol% capsule, $CDCl_3$, 50 °C, alox as additive]

The unusually mild reaction conditions, devoid of any strong hydrogen bond donor and acceptor, combined with the excellent, and substrate independent, β-selectivities observed, indicated that there might be more at work than a regular loose S_N2-mechanism. Due to their stability, glycoside fluorides usually require strong activation.[51] However, in the capsule catalyst, only hydrogen bonds from water and phenol groups are available. As mentioned in the section on control experiments, the closely related **PG** capsule **II** did not catalyse the glycosylation reaction (Fig. 3A, entry 6). This control experiment is important in the context of the mechanistic discussion, as it indicates that the sole encapsulation of the substrates is not sufficient for catalysis. In addition to encapsulation that is also observed in the **PG** capsule (see SI, page S11), an additional activation has to take place inside capsule **I**. It has been demonstrated that encapsulation can perturb the pK_a of guest molecules and accelerate reactions in other host systems.[58,59] For capsule **I**, an increased acidity of the capsule/increased basicity of the guest was reported.[33] However, this increased acidity (pK_a approx. 5.5-6) alone is not sufficient for the conversion observed, as demonstrated by the control experiment (Fig. 3A, entry 8) with acetic acid (pK_a approx. 5). Interestingly, all the hydrogen bonds of **I** are communicating, as a proton can be freely shifted over the whole network of 60 hydrogen bonds. This prompted us to postulate a synchronized activation of the electrophile and nucleophile by the hydrogen bond network (Fig. 1B). The electrophile requires a general acid, while the nucleophile depends on a general base for activation. A reciprocal proton transfer enabled via the capsule's hydrogen bond network may satisfy both reaction partners' requirements for activation.

To learn more about this potential activation mode in atomistic detail, we performed a QM/MM enhanced sampling molecular dynamics (metadynamics)[60,61] simulation. We defined a collective variable (CV) as an antisymmetric linear combination of the interatomic distances d_{Cl} (distance between the chloride leaving group and the anomeric carbon) and d_{Me} (distance between the anomeric carbon and the methanol oxygen nucleophile). The resulting CV, in the form d_{Cl}-d_{Me}, describes the nucleophilic substitution without any *a priori* assumption on the mechanism (see SI chapter 16). In Fig. 5A, we report the free energy profile of the reaction obtained by statistical

reweighting of the metadynamics trajectory. The left and right basins are associated to the reactant and product states respectively, and are separated by a free energy barrier of 48 kJ/mol (12 kcal/mol) and their relative free energy difference is approximately zero (see SI-Fig. S17 showing the convergent behavior of the free energy estimation). Overlayed to the free energy profile in Fig. 5, we report three representative structures for the reactant, transition, and product states, respectively. In the reactant state, the chlorine atom is hydrogen-bonded to a water molecule at a corner site of the capsule (Fig. 5A) as previously observed for a Friedel-Crafts reaction in static quantum chemical calculations by Neri and coworkers.[62] At the same time, the methanol OH group is dynamically hydrogen bonded to both the corner-sharing water molecule on the opposite side and to a phenol group. This particular arrangement is fundamental for enabling the reaction. To initiate the transition, water donates a proton to the chlorine atom and begins to abstract another one from an adjacent phenol group. After the cleavage of the carbon-chlorine bond, the hydrogen bond network between the leaving group and the nucleophile strengthens/rigidifies, thus, allowing at the same time the stabilization of the S_N2 transition structure and the fast proton migration from the methanol OH group to the leaving chloride anion. To further investigate the mechanistic aspects of the reaction, we calculated reactive quasi-classical trajectories (QCT, see for example[63,64]) starting from a transition structure extracted from the metadynamics trajectory (see Fig. 5B and SI for details). As described in a recent study,[65] we extracted two fundamental pieces of information from QCT. First, when the system is initialized at t=0 the difference between d_{Cl} and d_{Me} is small (0.1 Å) and varies concertedly during bond breaking and formation, indicating a synchronous S_N2 mechanism. It is worth noting that when the C-Cl bond is cleaved, the chloride anion is neutralized by a proton from a water molecule on the capsule's surface. This causes the non-monotonic increase of d_{Cl} in the QCT analysis. Second, we estimated the time gap between bond-cleavage ($d_{Cl} > 2.3$ Å) and bond-formation ($d_{Me} < 2.3$ Å). The median time of the transition corresponds to 529 fs, which is particularly long if compared to simpler reactions in the gas phase,[66,67] and compares well with recent literature findings,[65] indicating an "energetically concerted"[68,69] loose S_N2 transition state for which high levels of stereospecificity are expected. These observations are in accordance with the experimental findings (see above) and with theoretical investigations.[65]

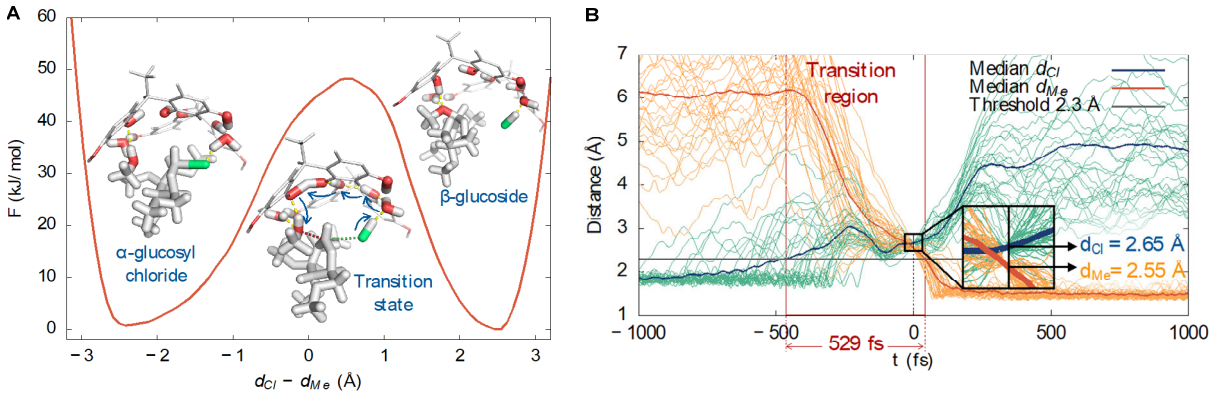

Figure 5. (A) Free energy profile for the reaction obtained by statistical reweighting of the metadynamics trajectory, and structures representing the reactants, transition state, and products. Color code: carbons (light grey); chlorine atom (green); oxygen (red); hydrogen (white). (B) QCT analysis for the d_{Cl} and d_{Me} distances, showing the transition region in pale red (starting when median $d_{Cl} > 2.3$ Å and median $d_{Me} < 2.3$ Å), and a magnification of the transition point at t=0 and the corresponding bond distances.

To gain some experimental insights into this mechanism, we decided to perform a proton inventory study.[70,71] Such experiments enable the identification of exchangeable protons that are involved in the rate-limiting step by generating a kinetic isotope effect. The study involves the measurement of the kinetic isotope effect at different deuterium/protium (D/H) ratios. The shape of the curve indicates the number of exchangeable protons involved in the rate-limiting step. Such studies have been used for the identification of proton wires.[70] A single participating proton would result in a linear relationship between the D/H ratio and k_H/k_D, while two protons would result in a quadratic relation. The reaction of **I** with **α-15** (Fig. 4E) does not follow a linear or a quadratic behavior, but rather an exponential progression (SI chapter 15.6). Such exponential curves indicate the participation of multiple exchangeable protons in the rate-limiting step, in agreement with the proton wire mechanism identified in the metadynamics simulations.

To conclude the mechanistic discussion, we summarize the key observations: (1) The unusually high β-selectivity cannot be rationalized by a conversion in solution, outside of the supramolecular capsule, as the extensive literature on glycosylation has demonstrated. (2) Rate-acceleration due to a high local concentration as a consequence of encapsulation of the substrates was excluded, as the closely related PG capsule that showed uptake of the reaction partners, did not lead to product formation. (3) Proton inventory studies indicated that more than two protic sites are involved in

the rate-limiting transition state. (4) The capsular network of hydrogen bonds would enable a communicating dual activation (proton wire) of the electrophile and the nucleophile. (5) QM/MM metadynamics simulations also indicated such a proton wire mechanism. Therefore, we conclude that a synchronized activation is the most likely mechanism in this catalyst system. A proton transfer over seven hydrogen bonds (Fig. 1B) elegantly satisfies the opposing catalytic requirements of the nucleophile and electrophile. Intriguingly, this mechanism is reminiscent of invertive cellulases[26] that also link a general base and a general acid via a proton relay (Fig. 1A). Although such mechanisms are known in nature, to our knowledge they have not been reported for man-made catalysts before.

Substrate scope

After having identified the likely mechanism, several further nucleophiles were explored (Fig. 6A). Besides primary alcohols, also more hindered secondary alcohols, specifically cyclohexanol and methyl lactate, were explored. For all mannosylations (**16a-e**), excellent β-selectivities were observed, and in most cases the α-isomer was barely detectable in the crude reaction mixture by ^{1}H NMR (α:β < 5:95). Even more interestingly, the reaction conditions were also applicable to alternative glycosyl donors. For instance, L-rhamnosyl fluoride also delivered the β-products (**17a-e**), again a 1,2-*cis* substitution pattern, in high selectivity. The reaction conditions were furthermore applicable to the 2-deoxy substrates. 2-Deoxy substrates are inherently challenging due to the lack of the C2-substituent able to direct the anomeric selectivity.[72] For both electrophiles investigated, 2-deoxy-D-glucosyl fluoride and 2-deoxy-D-galactosyl fluoride, excellent β-selectivities and generally very high yields were observed (**18a-e**, **19a-e**). To complete the electrophile scope, also the formation of 1,2-*trans* substituted products (**13a-e**, **20a-e**) was explored. D-Glucosyl chloride and D-galactosyl fluoride were glycosylated with all five nucleophiles in excellent β-selectivity and yields. In the case of the D-glucosyl chloride, the match/mismatch situation with the enantiomeric nucleophiles, methyl (*S*)-lactate and (*R*)-lactate, was explored. Both nucleophiles gave excellent β-diastereoselectivities (7:93 and <5:95). After having demonstrated the broad scope of glycoside donors, the scope of nucleophiles was extended (Fig. 6B). A whole variety of primary alcohols, carrying sensitive functionalities like an alkyl bromide (**13i**), epoxide (**13k**), or an acetal (**13l**) were successfully attached in excellent β-

selectivity. The limitations became visible with the weak nucleophile 2,2,2-trifluoroethanol (**13g**) that resulted in a reduced yield (32%) under the standard reaction conditions. A lower yield (34%) was also obtained for the product containing an epoxide moiety (**13k**).

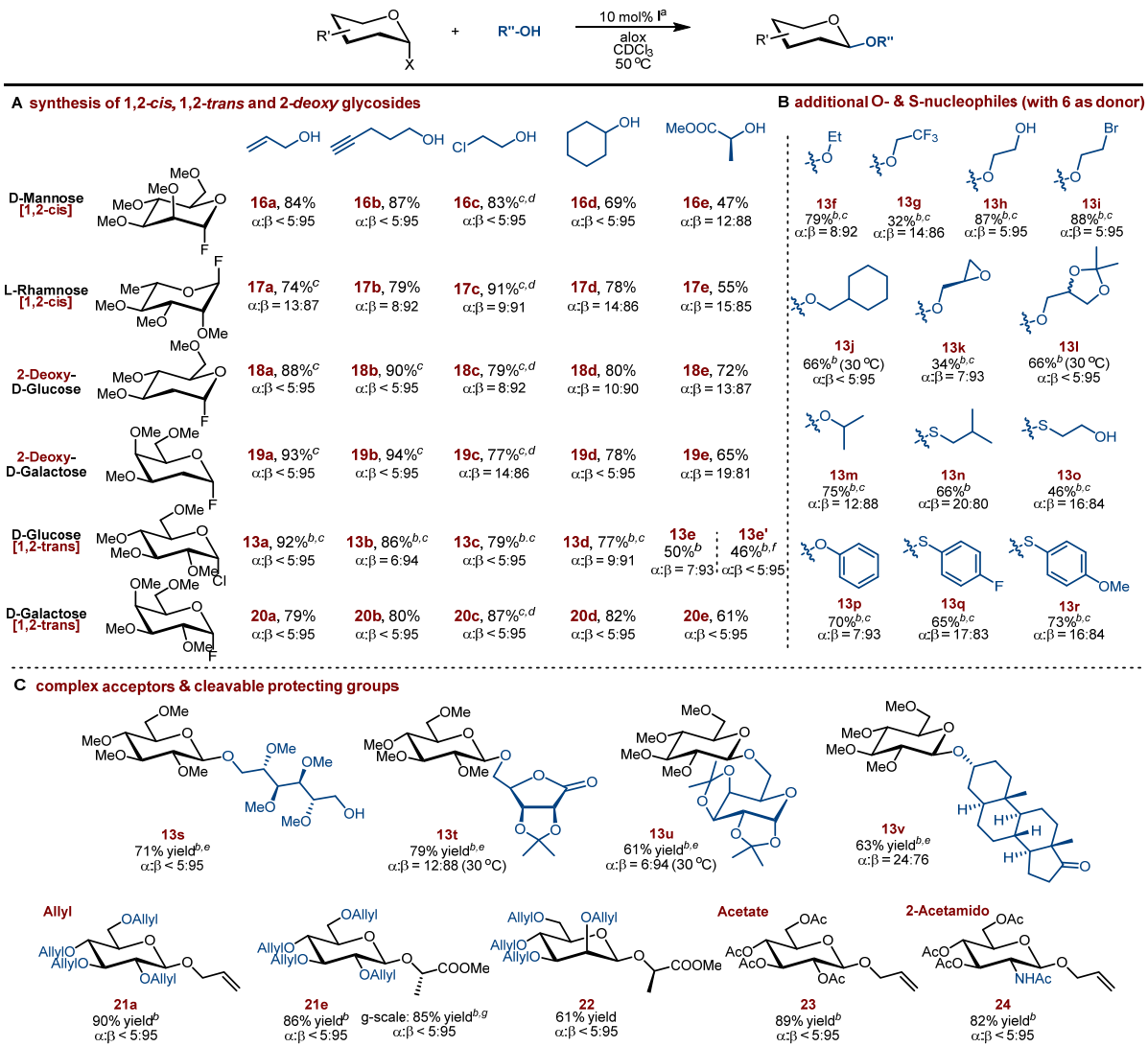

Figure 6. (A) Substrate table describing the scope of the unified approach for the selective construction of *cis*-1,2-, 2-deoxy-, and *trans*-1,2- β-glycosidic linkages. (B) Additional oxygen- and sulfur-nucleophiles were explored. (C) Complex nucleophiles and cleavable protecting groups were explored that delivered disaccharides and fully deprotectable products in excellent β-selectivity. [a]Unless noted otherwise, reactions were performed with glycosyl fluoride (100 µmol, 1.0 equiv.), nucleophile (500 µmol, 5.0 equiv.), capsule (66.3 mg, 10 mol%), alox (100 mg) in $CDCl_3$ (1.00 mL) at 50 °C; Isolated yields; Diastereomeric ratios were determined by ^1H NMR of

the reaction mixture. [b]Glucosyl chloride was used instead of the corresponding fluoride. [c]Reactions were performed at 20 °C. [d]alox basic was used instead of alox neutral. [e]3.0 equivalents of acceptor were used. [f]Methyl (R)-lactate was used. [g] large scale reaction was performed in $CHCl_3$

Moreover, phenol, thiol, and thiophenol nucleophiles proved to be suitable glycosyl acceptors (**13n**-**13r**, Fig. 6B), making this transformation useful for the preparation of known saccharide donors.[73]

Finally, the use of larger, more complex nucleophiles was explored (Fig. 6C). Tetramethyl D-mannitol delivered the disaccharide product **13s** in excellent diastereoselectivity. Also 2,3-O-isopropylidene-D-ribonic γ-lactone and 1,2:3,4-Di-O-isopropylidene-α-D-galactopyranose worked well as nucleophiles, yielding products **13t** and **13u** in good yields and excellent selectivity. Due to the size limitation inside **I**, no fully deprotectable disaccharide can be accessed. To explore the size limits of the glycosylation inside the cavity of **I**, we turned to a steroid nucleophile. Androsterone was converted to the glycoside **13v**, in slightly reduced β-selectivity. Molecular modeling (see SI, page S66) indicates that the reagents indeed fill most of the cavity space available. In total, 37 heavy atoms (carbon, oxygen, chlorine) have to be encapsulated to perform this reaction inside the capsule. This is close to the size limitation for reactions inside of **I**, in agreement with encapsulation studies of tetraalkyl ammonium guests.[28]

After having explored the substrate scope with methylated donors, the use of cleavable protecting groups was investigated (Fig. 6C). Due to the reaction taking place inside the confined space of capsule **I** (approx. 1400 $Å^3$), there are obviously limits concerning the reactants' sizes. Nevertheless, both allyl and acetate protecting groups are tolerated very well, providing the products **21a**, **21e**, **22**, and **23** in good yields and excellent diastereoselectivity (α:β < 5:95). The synthesis of β-glucoside **21e** was also performed on gram scale. It was isolated in 85% yield (1.09g) and excellent β-selectivity, demonstrating the scalability of the procedure. Importantly, catalyst **I** can be easily recovered by a simple precipitation procedure (see SI chapter 9), and used at least six times without any loss in activity and selectivity. Furthermore, the protecting groups in **21e** were cleaved to deliver the unprotected β-D-glucose derivative **S-8** (see SI, page S58). The challenging 2-acetamido substrate substitution pattern was also explored. This pattern usually leads to unreactive oxazoline intermediates, requiring alternative protecting groups for the nitrogen

at C2.[38] In contrast, with the capsule catalyst clean formation of the β-substituted product **24** in excellent selectivity was observed, further underscoring the versatility of this catalyst system.

Synthesis of known β-saccharides

To demonstrate the applicability of the catalyst for the synthesis of known β-glycosides, two 2-deoxy compounds were synthesized. β-Nonyl 2-deoxy arabinose **27** (Fig. 7A) was chosen as a target as it displays mesomorphic behavior, in contrast to its α-isomer.[74] In the literature, it was prepared from a thioglycoside donor that was activated with stoichiometric amounts of N-iodosuccinimide and catalytic amounts of trimethylsilyl trifluoromethanesulfonate (TMSOTf), failing to induce stereoselectivity (both isomers were formed in 30-35% yield).[74] The methodology presented in this paper yielded a high β-selectivity (10:90) in the glycosylation of the allyl protected glycosyl fluoride **25**. Product **26** was obtained in 70% yield and was successfully deprotected to deliver the mesomorphic compound **27**. Additionally, also the potent anti-tumor agent **31** (Fig. 7B)[75] was readily accessible with the methodology developed. The key step delivered the β-glycoside **28** in high yield (71%) and excellent selectivity (α:β = 7:93). After acetal cleavage, first the primary and subsequently the secondary alcohols were alkylated to deliver **30**. A final deprotection delivered the anti-tumor agent **31** in excellent overall yield and diastereoselectivity. The synthesis developed compares favourably to the literature route that relies on the anchimeric assistance of a 2-acetoxy group for β-selectivity. The required acetoxy group had to be removed subsequently in a lengthy procedure (three steps), leading to a long synthetic sequence of ten linear steps, and fifteen total steps.[75] The methodology presented here enabled the synthesis of **31** in only eight total steps.

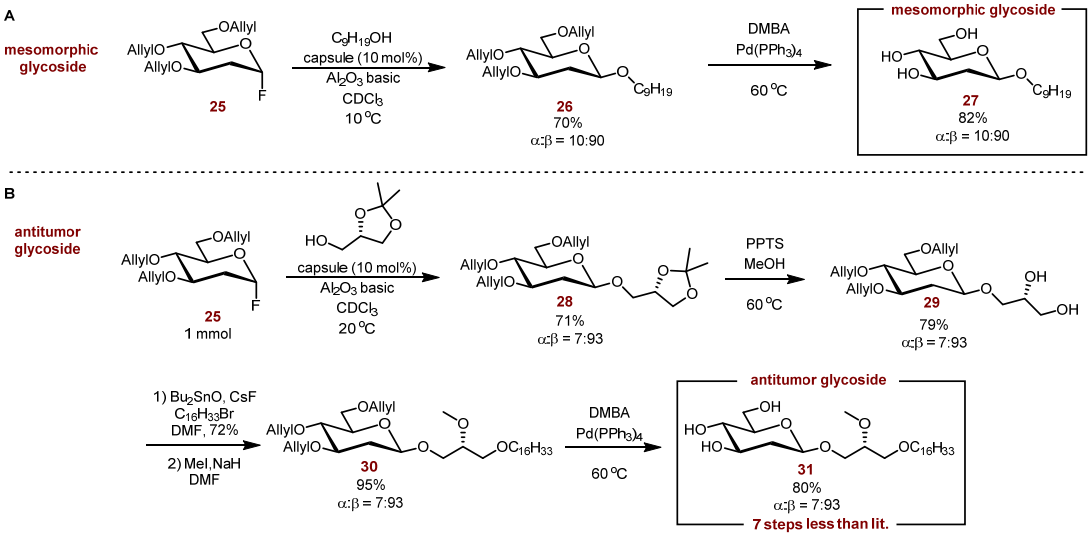

Figure 7. (A) Application of the methodology for the β-selective synthesis of the mesomorphic glycoside **27**. (B) Application of the methodology for the β-selective synthesis of the anti-tumor agent **31**. DMBA: 1,3-dimethylbarbituric acid.

Summary

We report strong evidence for a proton wire-enabled dual activation mode inside the supramolecular capsule **I**. While such a mechanism has been identified in enzymes, to our knowledge, it is novel for man-made catalysts. This mechanism enables the activation of glycosyl chlorides and even fluorides at ambient or slightly elevated temperatures (50 °C), although no strong hydrogen bond donors or acceptors are present. The activation is achieved solely by hydrogen bonding of water molecules and phenol moieties that are part of the molecular container. Control experiments provided very strong evidence that the selective glycosylations take place inside the capsule's cavity. Consistent with these results, size-selective glycosylation was achieved for the first time with a man-made catalyst.

Catalyst **I** is commercially available or readily prepared in large quantities (>300g batches) in one single step, and displays excellent β-selectivity for *cis*-1,2-, *trans*-1,2-, and 2-deoxy-products, as long as the substrates fit the cavity of the capsule. The glycosylation reaction is scalable without a loss in yield or diastereoselectivity. The catalyst can be readily recycled by a simple precipitation procedure and used at least six times without any loss in activity and selectivity. The reaction

conditions are compatible with a wide range of functional groups, including alkenes, alkynes, alkyl chlorides and bromides, esters, alcohols, acetals, allyl ethers, amides, ketones, as well as epoxides. Due to the ready availability of the catalyst and the excellent β-selectivities obtained for a wide range of donors and acceptors, we expect the methodology to be useful to the community. As first applications, two known 2-deoxy saccharides with physicochemical or biological functions were efficiently prepared via this methodology. We are confident that this finding will stimulate the discovery of further powerful glycosylation catalysts relying on this synchronized proton wire activation mode.

References

1 Kirby, A. J. Enzyme mechanisms, models, and mimics. *Angew. Chem. Int. Ed.* **35**, 707-724 (1996).

2 Motherwell, W. B., Bingham, M. J. & Six, Y. Recent progress in the design and synthesis of artificial enzymes. *Tetrahedron* **57**, 4663-4686, doi:Doi 10.1016/S0040-4020(01)00288-5 (2001).

3 Breslow, R. & Dong, S. D. Biomimetic Reactions Catalyzed by Cyclodextrins and Their Derivatives. *Chem. Rev.* **98**, 1997-2012, doi:10.1021/cr970011j (1998).

4 Hof, F., Craig, S. L., Nuckolls, C. & Rebek, J. J. Molecular Encapsulation. *Angew. Chem. Int. Ed.* **41**, 1488-1508, doi:10.1002/20020503 (2002).

5 Koblenz, T. S., Wassenaar, J. & Reek, J. N. H. Reactivity within a confined self-assembled nanospace. *Chem. Soc. Rev.* **37**, 247-262, doi: 10.1039/B614961h (2008).

6 Rebek, J. Molecular Behavior in Small Spaces. *Acc. Chem. Res.* **42**, 1660-1668, doi: 10.1021/Ar9001203 (2009).

7 Yoshizawa, M., Klosterman, J. K. & Fujita, M. Functional Molecular Flasks: New Properties and Reactions within Discrete, Self-Assembled Hosts. *Angew. Chem. Int. Ed.* **48**, 3418-3438, doi: 10.1002/anie.200805340 (2009).

8 Wiester, M. J., Ulmann, P. A. & Mirkin, C. A. Enzyme Mimics Based Upon Supramolecular Coordination Chemistry. *Angew. Chem. Int. Ed.* **50**, 114-137, doi: 10.1002/anie.201000380 (2011).

9 Conn, M. M. & Rebek, J. Self-Assembling Capsules. *Chem. Rev.* **97**, 1647-1668, doi:10.1021/cr9603800 (1997).

10 Hong, C. M., Bergman, R. G., Raymond, K. N. & Toste, F. D. Self-Assembled Tetrahedral Hosts as Supramolecular Catalysts. *Acc. Chem. Res.* **51**, 2447-2455, doi:10.1021/ 8b00328 (2018).

11 Zhang, Q., Catti, L. & Tiefenbacher, K. Catalysis inside the Hexameric Resorcinarene Capsule. *Acc. Chem. Res.* **51**, 2107-2114, doi:10.1021/acs.accounts.8b00320 (2018).

12 Gaeta, C. *et al.* The Hexameric Resorcinarene Capsule at Work: Supramolecular Catalysis in Confined Spaces. *Chem. Eur. J.* **25**, 4899-4913, doi:10.1002/chem.201805206 (2019).

13 Mouarrawis, V., Plessius, R., van der Vlugt, J. I. & Reek, J. N. H. Confinement Effects in Catalysis Using Well-Defined Materials and Cages. *Front. Chem.* **6**, doi:10.3389/fchem.2018.00623 (2018).

14 Ward, M. D., Hunter, C. A. & Williams, N. H. Coordination Cages Based on Bis(pyrazolylpyridine) Ligands: Structures, Dynamic Behavior, Guest Binding, and Catalysis. *Acc. Chem. Res.* **51**, 2073-2082, doi:10.1021/acs.accounts.8b00261 (2018).

15 Némethová, I., Syntrivanis, L.-D. & Tiefenbacher, K. Molecular Capsule Catalysis: Ready to Address Current Challenges in Synthetic Organic Chemistry? *CHIMIA* **74**, 561-568, doi:10.2533/chimia.2020.561 (2020).

16 Kang, J. & Rebek, J. Acceleration of a Diels-Alder reaction by a self-assembled molecular capsule. *Nature* **385**, 50-52 (1997).
17 Yoshizawa, M., Tamura, M. & Fujita, M. Diels-Alder in Aqueous Molecular Hosts: Unusual Regioselectivity and Efficient Catalysis. *Science* **312**, 251-254, doi:10.1126/science.1124985 (2006).
18 Ajami, D. & Rebek, J. More Chemistry in Small Spaces. *Acc. Chem. Res.* **46**, 990-999, doi:10.1021/ar300038r (2012).
19 Leenders, S. H. A. M., Gramage-Doria, R., de Bruin, B. & Reek, J. N. H. Transition metal catalysis in confined spaces. *Chem. Soc. Rev.* **44**, 433-448, doi:10.1039/C4CS00192C (2015).
20 Raynal, M., Ballester, P., Vidal-Ferran, A. & van Leeuwen, P. W. N. M. Supramolecular catalysis. Part 2: artificial enzyme mimics. *Chem. Soc. Rev.* **43**, 1734-1787, doi:10.1039/C3CS60037H (2014).
21 Catti, L., Zhang, Q. & Tiefenbacher, K. Advantages of Catalysis in Self-Assembled Molecular Capsules. *Chem. - Eur. J.* **22**, 9060-9066, doi:10.1002/chem.201600726 (2016).
22 Morimoto, M. *et al.* Advances in supramolecular host-mediated reactivity. *Nat. Catal.* **3**, 969-984, doi:10.1038/s41929-020-00528-3 (2020).
23 Percástegui, E. G., Ronson, T. K. & Nitschke, J. R. Design and Applications of Water-Soluble Coordination Cages. *Chem. Rev.* **120**, 13480-13544, doi:10.1021/acs.chemrev.0c00672 (2020).
24 Frank, R. A. W., Titman, C. M., Pratap, J. V., Luisi, B. F. & Perham, R. N. A Molecular Switch and Proton Wire Synchronize the Active Sites in Thiamine Enzymes. *Science* **306**, 872, doi:10.1126/science.1101030 (2004).
25 Cukierman, S. Et tu, Grotthuss! and other unfinished stories. *Biochim. Biophys. Acta Bioenerg.* **1757**, 876-885, doi:https://doi.org/10.1016/j.bbabio.2005.12.001 (2006).
26 Nakamura, A. *et al.* "Newton's cradle" proton relay with amide–imidic acid tautomerization in inverting cellulase visualized by neutron crystallography. *Sci. Adv.* **1**, e1500263, doi:10.1126/sciadv.1500263 (2015).
27 MacGillivray, L. R. & Atwood, J. L. A chiral spherical molecular assembly held together by 60 hydrogen bonds. *Nature* **389**, 469-472, doi:http://www.nature.com/nature/journal/v389/n6650/suppinfo/389469a0_S1.html (1997).
28 Shivanyuk, A. & Rebek, J. Reversible encapsulation by self-assembling resorcinarene subunits. *Proc. Natl. Acad. Sci. USA* **98**, 7662-7665, doi:10.1073/pnas.141226898 (2001).
29 Avram, L. & Cohen, Y. Spontaneous Formation of Hexameric Resorcinarene Capsule in Chloroform Solution as Detected by Diffusion NMR. *J. Am. Chem. Soc.* **124**, 15148-15149, doi:10.1021/ja0272686 (2002).
30 Avram, L., Cohen, Y. & Rebek, J. Recent advances in hydrogen-bonded hexameric encapsulation complexes. *Chem. Commun.* **47**, 5368-5375, doi:10.1039/c1cc10150a (2011).
31 Bianchini, G., La Sorella, G., Canever, N., Scarso, A. & Strukul, G. Efficient isonitrile hydration through encapsulation within a hexameric self-assembled capsule and selective inhibition by a photo-controllable competitive guest. *Chem. Commun.* **49**, 5322-5324, doi:Doi 10.1039/C3cc42233j (2013).
32 Cavarzan, A., Scarso, A., Sgarbossa, P., Strukul, G. & Reek, J. N. H. Supramolecular Control on Chemo- and Regioselectivity via Encapsulation of (NHC)-Au Catalyst within a Hexameric Self-Assembled Host. *J. Am. Chem. Soc.* **133**, 2848-2851, doi:10.1021/ja111106x (2011).
33 Zhang, Q. & Tiefenbacher, K. Hexameric Resorcinarene Capsule is a Brønsted Acid: Investigation and Application to Synthesis and Catalysis. *J. Am. Chem. Soc.* **135**, 16213-16219, doi:10.1021/ja4080375 (2013).

34 Köster, J. M. & Tiefenbacher, K. Elucidating the Importance of Hydrochloric Acid as a Cocatalyst for Resorcinarene-Capsule-Catalyzed Reactions. *ChemCatChem* **10**, 2941-2944, doi:doi:10.1002/cctc.201800326 (2018).
35 Merget, S., Catti, L., Piccini, G. & Tiefenbacher, K. Requirements for Terpene Cyclizations inside the Supramolecular Resorcinarene Capsule: Bound Water and Its Protonation Determine the Catalytic Activity. *J. Am. Chem. Soc.* **142**, 4400-4410, doi:10.1021/jacs.9b13239 (2020).
36 Tanaka, Y., Khare, C., Yonezawa, M. & Aoyama, Y. Highly stereoselective glycosidation of ribose solubilized in apolar organic media via host-guest complexation1. *Tetrahedron Lett.* **31**, 6193-6196, doi:https://doi.org/10.1016/S0040-4039(00)97022-9 (1990).
37 Zhu, X. & Schmidt, R. R. New Principles for Glycoside-Bond Formation. *Angew. Chem. Int. Ed.* **48**, 1900-1934, doi:10.1002/anie.200802036 (2009).
38 Nigudkar, S. S. & Demchenko, A. V. Stereocontrolled 1,2-cis glycosylation as the driving force of progress in synthetic carbohydrate chemistry. *Chem. Sci.* **6**, 2687-2704, doi:10.1039/C5SC00280J (2015).
39 Jensen, K. J. O-Glycosylations under neutral or basic conditions. *J. Chem. Soc., Perkin Trans. 1*, 2219-2233, doi:10.1039/B110071H (2002).
40 Davis, B. G. Recent developments in oligosaccharide synthesis. *J. Chem. Soc., Perkin Trans. 1*, 2137-2160, doi:10.1039/A809774G (2000).
41 Das, R. & Mukhopadhyay, B. Chemical O-Glycosylations: An Overview. *ChemistryOpen* **5**, 401-433, doi:10.1002/open.201600043 (2016).
42 Ling, J. & Bennett, C. S. Recent Developments in Stereoselective Chemical Glycosylation. *Asian J. Org. Chem.* **8**, 802-813, doi:10.1002/ajoc.201900102 (2019).
43 Nielsen, M. M. & Pedersen, C. M. Catalytic Glycosylations in Oligosaccharide Synthesis. *Chem. Rev.* **118**, 8285-8358, doi:10.1021/acs.chemrev.8b00144 (2018).
44 McKay, M. J. & Nguyen, H. M. Recent Advances in Transition Metal-Catalyzed Glycosylation. *ACS Catal.* **2**, 1563-1595, doi:10.1021/cs3002513 (2012).
45 Li, W. & Yu, B. Gold-catalyzed glycosylation in the synthesis of complex carbohydrate-containing natural products. *Chem. Soc. Rev.* **47**, 7954-7984, doi:10.1039/C8CS00209F (2018).
46 Williams, R. & Galan, M. C. Recent Advances in Organocatalytic Glycosylations. *Eur. J. Org. Chem.* **2017**, 6247-6264, doi:https://doi.org/10.1002/ejoc.201700785 (2017).
47 Crich, D. Mechanism of a Chemical Glycosylation Reaction. *Acc. Chem. Res.* **43**, 1144-1153, doi:10.1021/ar100035r (2010).
48 Adero, P. O., Amarasekara, H., Wen, P., Bohé, L. & Crich, D. The Experimental Evidence in Support of Glycosylation Mechanisms at the SN1–SN2 Interface. *Chem. Rev.* **118**, 8242-8284, doi:10.1021/acs.chemrev.8b00083 (2018).
49 Park, Y. *et al.* Macrocyclic bis-thioureas catalyze stereospecific glycosylation reactions. *Science* **355**, 162-166, doi:10.1126/science.aal1875 (2017).
50 Kwan, E. E., Park, Y., Besser, H. A., Anderson, T. L. & Jacobsen, E. N. Sensitive and Accurate 13C Kinetic Isotope Effect Measurements Enabled by Polarization Transfer. *J. Am. Chem. Soc.* **139**, 43-46, doi:10.1021/jacs.6b10621 (2017).
51 Mukaiyama, T. & Jona, H. Glycosyl fluoride A superb glycosyl donor in glycosylation. *Proc. Jpn. Acad. B: Phys. Biol. Sci.* **78**, 73-83, doi:10.2183/pjab.78.73 (2002).
52 Gerkensmeier, T. *et al.* Self-assembly of 2,8,14,20-tetraisobutyl-5,11,17,23-tetrahydroxyresorc[4]arene. *Eur. J. Org. Chem.*, 2257-2262 (1999).
53 Zhang, Q., Catti, L., Kaila, V. R. I. & Tiefenbacher, K. To catalyze or not to catalyze: elucidation of the subtle differences between the hexameric capsules of pyrogallolarene and resorcinarene. *Chem. Sci.* **8**, 1653-1657, doi:10.1039/C6SC04565K (2017).

54 Crich, D. & Chandrasekera, N. S. Mechanism of 4,6-O-Benzylidene-Directed β-Mannosylation as Determined by α-Deuterium Kinetic Isotope Effects. *Angew. Chem. Int. Ed.* **43**, 5386-5389, doi:10.1002/anie.200453688 (2004).
55 Matsui, H., Blanchard, J. S., Brewer, C. F. & Hehre, E. J. Alpha-secondary tritium kinetic isotope effects for the hydrolysis of alpha-D-glucopyranosyl fluoride by exo-alpha-glucanases. *J. Biol. Chem.* **264**, 8714-8716 (1989).
56 Chan, J., Sannikova, N., Tang, A. & Bennet, A. J. Transition-State Structure for the Quintessential SN2 Reaction of a Carbohydrate: Reaction of α-Glucopyranosyl Fluoride with Azide Ion in Water. *J. Am. Chem. Soc.* **136**, 12225-12228, doi:10.1021/ja506092h (2014).
57 Slovak, S. & Cohen, Y. The Effect of Alcohol Structures on the Interaction Mode with the Hexameric Capsule of Resorcin[4]arene. *Chem. – Eur. J.* **18**, 8515-8520, doi:10.1002/chem.201102809 (2012).
58 Wang, K. *et al.* Electrostatic Control of Macrocyclization Reactions within Nanospaces. *J. Am. Chem. Soc.* **141**, 6740-6747, doi:10.1021/jacs.9b02287 (2019).
59 Cai, X., Kataria, R. & Gibb, B. C. Intrinsic and Extrinsic Control of the pKa of Thiol Guests inside Yoctoliter Containers. *J. Am. Chem. Soc.* **142**, 8291-8298, doi:10.1021/jacs.0c00907 (2020).
60 Barducci, A., Bussi, G. & Parrinello, M. Well-Tempered Metadynamics: A Smoothly Converging and Tunable Free-Energy Method. *Phys. Rev. Lett.* **100**, 020603, doi:10.1103/PhysRevLett.100.020603 (2008).
61 Grifoni, E., Piccini, G. & Parrinello, M. Microscopic description of acid–base equilibrium. *Proc. Natl. Acad. Sci. USA* **116**, 4054, doi:10.1073/pnas.1819771116 (2019).
62 La Manna, P. *et al.* Mild Friedel–Crafts Reactions inside a Hexameric Resorcinarene Capsule: C–Cl Bond Activation through Hydrogen Bonding to Bridging Water Molecules. *Angew. Chem. Int. Ed.* **57**, 5423-5428, doi:https://doi.org/10.1002/anie.201801642 (2018).
63 Doubleday, C., Bolton, K. & Hase, W. L. Direct Dynamics Quasiclassical Trajectory Study of the Thermal Stereomutations of Cyclopropane. *J. Phys. Chem. A* **102**, 3648-3658, doi:10.1021/jp973273y (1998).
64 Xu, L., Doubleday, C. E. & Houk, K. N. Dynamics of 1,3-Dipolar Cycloadditions: Energy Partitioning of Reactants and Quantitation of Synchronicity. *J. Am. Chem. Soc.* **132**, 3029-3037, doi:10.1021/ja909372f (2010).
65 Fu, Y., Bernasconi, L. & Liu, P. Ab Initio Molecular Dynamics Simulations of the SN1/SN2 Mechanistic Continuum in Glycosylation Reactions. *J. Am. Chem. Soc.* **143**, 1577-1589, doi:10.1021/jacs.0c12096 (2021).
66 Xu, L., Doubleday, C. E. & Houk, K. N. Dynamics of 1,3-Dipolar Cycloaddition Reactions of Diazonium Betaines to Acetylene and Ethylene: Bending Vibrations Facilitate Reaction. *Angew. Chem. Int. Ed.* **48**, 2746-2748, doi:https://doi.org/10.1002/anie.200805906 (2009).
67 Jiménez-Osés, G., Liu, P., Matute, R. A. & Houk, K. N. Competition Between Concerted and Stepwise Dynamics in the Triplet Di-π-Methane Rearrangement. *Angew. Chem. Int. Ed.* **53**, 8664-8667, doi:https://doi.org/10.1002/anie.201310237 (2014).
68 Baldwin, J. E. & Fleming, R. H. Allene-olefin and allene-allene cycloadditions methylenecyclobutane and 1,2-dimethylenecyclobutane degenerate rearrangements 281-310 (Springer Berlin Heidelberg) doi: 10.1007/BFb0050819.
69 Patel, A. *et al.* Dynamically Complex [6+4] and [4+2] Cycloadditions in the Biosynthesis of Spinosyn A. *J. Am. Chem. Soc.* **138**, 3631-3634, doi:10.1021/jacs.6b00017 (2016).
70 Venkatasubban, K. S. & Schowen, R. L. The Proton Inventory Techniqu. *Crit. Rev. Biochem. Mol. Biol.* **17**, 1-44, doi:10.3109/10409238409110268 (1984).
71 Schowen, R. L. The use of solvent isotope effects in the pursuit of enzyme mechanisms. *J. Labelled Compd. Radiopharm.* **50**, 1052-1062, doi:https://doi.org/10.1002/jlcr.1436 (2007).

72 Bennett, C. S. & Galan, M. C. Methods for 2-Deoxyglycoside Synthesis. *Chem. Rev.* **118**, 7931-7985, doi:10.1021/acs.chemrev.7b00731 (2018).
73 Yao, H., Vu, M. D. & Liu, X.-W. Recent advances in reagent-controlled stereoselective/stereospecific glycosylation. *Carbohydr. Res.* **473**, 72-81, doi:https://doi.org/10.1016/j.carres.2018.10.006 (2019).
74 Singh, M. K., Jayaraman, N., Rao, D. S. S. & Prasad, S. K. Effect of the C-2 hydroxyl group on the mesomorphism of alkyl glycosides: synthesis and thermotropic behavior of alkyl 2-deoxy-d-arabino-hexopyranosides. *Chem. Phys. Lipids* **155**, 90-97, doi:https://doi.org/10.1016/j.chemphyslip.2008.07.008 (2008).
75 Marino-Albernas, J. R., Bittman, R., Peters, A. & Mayhew, E. Synthesis and Growth Inhibitory Properties of Glycosides of 1-O-Hexadecyl-2-O-methyl-sn-glycerol, Analogs of the Antitumor Ether Lipid ET-18-OCH3 (Edelfosine). *J. Med. Chem.* **39**, 3241-3247, doi:10.1021/jm960164j (1996).

Data availability The data that support the findings of this study are available online in the Supplementary Information (experimental procedures, characterization data, copies of the NMR spectra of novel compounds). The source data for the figures 2, 3, 4, 6, 7 will be deposited on Zenodo (https://zenodo.org/). Simulations input files for figure 5A-B will be uploaded on the PLUMED-NEST! repository (https://www.plumed-nest.org/).

Acknowledgments The authors thank Dr. Michael Pfeffer for HR-MS analysis and Prof. Thomas R. Ward for helpful discussions. Molecular dynamics calculations were carried on the ETH Zurich cluster Euler.

Funding This work was supported by the Swiss National Science Foundation as part of the NCCR Molecular Systems Engineering.

Author contributions K.T. conceived and supervised the project. K.T. and T.L. planned the project. T.L. carried out all the experiments except the mechanistic investigations concerning SKIE and reaction order, which were performed by F.H. T.L. and K.T. compiled the first draft of the manuscript. GM.P conceived and modelled the simulation of the system, carried out the simulations, interpreted the results, and wrote the first draft of the molecular dynamics section. All authors contributed to the final version of the manuscript.

Competing interests Authors declare no competing interests.